

# Quantum Dynamics of the HMF Model

Ryan Plestid\*

*Department of Physics and Astronomy, McMaster University, Hamilton, Ontario, Canada and  
Perimeter Institute for Theoretical Physics, Waterloo, Ontario, Canada*

Perry Mahon

*Department of Physics and Astronomy, McMaster University, Hamilton, Ontario, Canada and  
Department of Physics, University of Toronto, Toronto, Ontario, Canada*

Duncan O'Dell†

*Department of Physics and Astronomy, McMaster University, Hamilton, Ontario, Canada*

We study the dynamics of the quantized Hamiltonian Mean Field (HMF) model assuming a Bose-condensed gas in the  $N \rightarrow \infty$  limit. We characterize the full set of stationary states, and study the dynamics of the model numerically focussing on competition between classical and quantum effects. We make contact with the existing literature on the HMF model as a classical system, and stress universal features which can be inferred in the semi-classical limit. In particular we show that the characteristic chevrons studied in the classical model [1] also appear in the quantum dynamics, but are dressed by an interference pattern that can be described in terms of the Pearcey function.

## I. INTRODUCTION

The HMF (Hamiltonian Mean Field) model is a system that has served for over twenty years as a paradigm in the study of long-range interacting, many-body systems [1–5]. Long-range interactions introduce a variety of complications from the perspective of statistical mechanics, the most of which is the loss of additivity. This is responsible for phenomena such as non-concave entropies and, by proxy, negative specific heat, the gravo-thermal heat catastrophe [6], and the inequivalence of ensembles, a phenomena which has been observed in the generalized HMF model [3]. Studies of the long time behaviour of these systems have also revealed their tendency to remain out-of-equilibrium even at late times, . The HMF model has great utility because it explains these features of long-range interacting systems in a simple and analytically tractable way.

The model's simplicity has allowed for explicit comparisons between statistical-mechanical predictions and direct simulations of molecular dynamics. This feature has proven to be extremely valuable for evaluating new ideas concerning the description of long-range interacting systems, and has helped shed light on multiple phenomena that standard statistical mechanics fails to explain. In particular studies of HMF dynamics have revealed: a Hamiltonian structure underlying the model's quasi-stationary states [1], a weak breaking of ergodicity [7, 8], and the role of topology in long-range interacting systems [9–11].

The  $1-D$  HMF model considered in this paper can be defined on a ring of radius  $R$ , and describes  $N$  interacting particles. The interaction is pair-wise, with a potential

energy that varies as  $\cos(\theta_i - \theta_j)$ . The Hamiltonian can be written as

$$H = \sum_{i=1}^N \frac{L_i^2}{2mR^2} + \frac{\epsilon}{2N} \sum_{ij} \cos(\theta_i - \theta_j). \quad (1)$$

with  $\epsilon > 0$  ( $\epsilon < 0$ ) corresponding to the anti-ferromagnetic (ferromagnetic) case. The nomenclature in terms of magnetism that is popular in the HMF literature is a consequence of the interpretation of the model as an infinite-range  $XY$  model. The  $1/N$  scaling of the inter-particle potential preserves the extensivity of the Hamiltonian, and is known as the Kac prescription [4].

Only recently has the quantization of the model been considered. In Refs. [12, 13] the static configurations of the model were thoroughly studied in the quantum regime for both fermions and bosons using mean-field theory, however the dynamics of the model remain uninvestigated. In this paper we restrict ourselves to the bosonic case, and study the dynamics of this system in the context of a mean-field approximation.

The paper is organized as follows: In Section II we introduce the various equivalent formalisms for studying the mean-field behaviour of the HMF. Section III contains our analytic results relating to both the statics and dynamics of the model. Section IV gives an overview of some of our numerical results, as well as outlining the basic numerical procedure used. In Section IV C we comment on universal structures that appear in the dynamics of the HMF model. Finally in Section V we discuss possible future directions for the quantum HMF model.

## II. MEAN-FIELD DESCRIPTIONS

Although the HMF model is often referred to as a mean-field model, there is an important distinction in nomenclature that must be emphasized. The HMF model's

\* plestird@mcmaster.ca

† dodell@mcmaster.ca

Hamiltonian provides an exact description of a quantum many-body system. This means that, for pure states, at any time  $t$  the system is fully specified by a state vector  $|\psi(t)\rangle$  that has an associated wave-function  $\psi(\theta_1, \theta_2, \dots, \theta_N)$  that depends on the position of all  $N$  particles.

In the large  $N$  limit of the bosonic HMF model a simplifying assumption can be made regarding the state of the system. By assuming that  $\psi$  can be written as a product of single-particle wave-functions [i.e.  $\psi = \prod_{i=1}^N \varphi(\theta_i)$ ] one can describe the  $N$  particle system by a single function of one variable. This is what constitutes the mean-field approximation in our analysis, and it arises naturally when treating a Bose-Einstein Condensate [14].

For classical systems ( $\hbar = 0$ ) with long-range interactions it has been rigorously shown that the mean-field description of the dynamics, in terms of the Vlasov equation, is exact in the  $N \rightarrow \infty$  limit [15]. This has not been rigorously shown for the corresponding case of quantum many-body systems, however qualitatively one should expect mean-field theory to approximate long-range interacting systems better than those with short-range interactions. This is because the potential's range allows a direct mechanism by which correlations can form over long distances. Additionally work on the charged-Coulomb gas in  $3 - D$  have shown that the mean-field treatment is validated in the limit of high-density limit when the specific small compared to the Bohr radius  $v \ll a_0^3$  [16]. This stands in contrast to short-range interacting Bose gases, where mean-field treatments apply for extremely dilute samples [14]. Despite these suggestions that mean-field theory should remain a good approximation for the treatment of long-range interacting quantum systems, the validity of the mean-field approximation is not guaranteed. The quantum HMF model's mean field description is discussed in detail in Refs. [12, 13]. For bosons, a mean-field treatment is equivalent to the *a priori* assumption of a Bose-Einstein condensate.

### A. Generalized Gross-Pitaevskii Equation

The mean-field treatment of a Bose-Einstein condensate is well established. Typically, the realistic, and therefore complicated, two-body potential in a problem can be replaced with a pseudo-potential, which reproduces the same low-energy scattering behaviour. The long-range nature of the two-body potential in the HMF model renders this procedure unsensible, and consequently the Gross-Pitaevskii equation (GPE) must be generalized. This can be referred to as the Generalized Gross-Pitaevskii equation (GGPE), as is the case in the dipolar atomic gas community, or as the Mean-Field Schrödinger Equation (MFSE) as found in Ref. [12]. This equation describes the evolution of the mean-field order parameter  $\Psi$  in terms of a non-local classical field theory.

The well known Gross-Pitaevskii equation is given by

$$i\hbar\partial_t\Psi = -\frac{\hbar^2}{2mR^2}\partial_\theta^2\Psi + g|\Psi|^2\Psi \quad (2)$$

where  $g$  is related to the s-wave scattering length  $a$  via  $g = (4\pi\hbar^2/m)a$ . This can be considered a special case of the GGPE shown in Eq. (3b) with  $\epsilon \rightarrow g$  and  $V(x) \rightarrow \delta(x)$ . To obtain the GGPE the  $|\Psi|^2\Psi$  term of the GPE is replaced by a mean-field potential that is determined self-consistently.

$$i\hbar\partial_t\Psi = -\frac{\hbar^2}{2mR^2}\partial_\theta^2\Psi + \epsilon\Phi(\theta, t)\Psi \quad (3a)$$

$$\Phi(\theta, t) = \int_{-\pi}^{\pi} |\Psi(\theta', t)|^2 \cos(\theta - \theta') d\theta' \quad (3b)$$

By rescaling  $t \rightarrow \hbar/(2mR^2)\tau$  the Eq. (3a) can be rewritten in terms of only one free parameter  $\chi^{-2} = \frac{\epsilon m R^2}{\hbar^2}$  which can be thought of as a reduced Planck's constant. It should be emphasized that despite being expressed as a square  $\chi^{-2}$  can take on negative values and its sign inherited from  $\epsilon$ . The positivity of  $\chi^{-2}$  is therefore related to whether we are discussing the ferromagnetic, or anti-ferromagnetic case. Written in terms of  $\chi^{-2}$  the GGPE takes the form

$$i\partial_\tau\Psi = -\partial_\theta^2\Psi + 2\chi^{-2}\Phi(\theta, t)\Psi \quad (4a)$$

$$\Phi(\theta, t) = \int_{-\pi}^{\pi} |\Psi(\theta', t)|^2 \cos(\theta - \theta') d\theta'. \quad (4b)$$

Due to the presence of the convolution in the definition of the mean-field potential  $\Phi$  it is convenient to work in the basis of Fourier modes. In this basis the GGPE takes the form

$$i\partial_\tau a_k = k^2 a_k + 2\chi^{-2} B_{kk'} a_{k'} \quad (5a)$$

$$B_{kk'} = \frac{1}{2} (\mathbf{M} \delta_{k+1, k'} + \mathbf{M}^* \delta_{k, k'+1}) \quad (5b)$$

$$\mathbf{M} = \sum_{\mathbb{Z}} a_k^* a_{k+1} = \int_{-\pi}^{\pi} |\Psi(\theta)|^2 e^{i\theta} d\theta \quad (5c)$$

The Fourier representation of the mean-field potential shows that in position space the potential can be written as  $1/2(\mathbf{M}^* e^{i\theta} + \mathbf{M} e^{-i\theta})$ . If we define  $\mathbf{M} = M e^{i\varphi}$ , it becomes manifest that the mean-field potential's representation in real space can be written as

$$\Phi(\theta, \tau) = M \cos(\theta - \varphi). \quad (6)$$

Both  $M$  and  $\varphi$  have depend implicitly on time through the order parameter (see Eq. (5c)). It follows that the mean-field potential is always a sinusoid, whose amplitude and minimum vary in time. This time-dependence must be determined self-consistently via the GGPE outlined above.

## B. Quantum Euler Equations

Defining  $\Psi = \sqrt{\rho} e^{iS/\hbar}$  we can transform Eq. (3a) into two coupled equations describing the evolution of the density  $\rho$  and a velocity profile which can be expressed as the gradient of the phase  $v = \frac{1}{\hbar} \partial_\theta S/m$ . Written in terms of these hydrodynamical variables, the equations read

$$\partial_t \rho + \frac{1}{R} \partial_\theta (\rho v) = 0 \quad (7a)$$

$$\partial_t v + \frac{1}{R} v \partial_\theta v + \frac{\epsilon}{mR} \partial_\theta \Phi = \partial_\theta \left( \frac{\hbar^2}{2m^2 R^2} \frac{\partial_\theta^2 \sqrt{\rho}}{\sqrt{\rho}} \right). \quad (7b)$$

The expression on the right-hand side is often referred to as the quantum pressure; here it is written as the gradient of Bohm's quantum potential. The description in terms of hydrodynamical variables is intimately linked with the assumption of a condensate. This hypothesis allows us to completely describe the system via a single density and phase; this would not be possible for a generic many-body wave-function.

To re-cast the equations in terms of  $\chi^{-2}$  we can take Eq. (4a) and re-scale  $\tau \rightarrow \frac{1}{2\chi} \mathcal{T}$  leading to

$$i\chi \partial_{\mathcal{T}} \Psi = -\frac{\chi^2}{2} \partial_\theta^2 \Psi + \Phi \Psi \quad (8)$$

and so we can treat this in the same manner as the unscaled GGPE with the identification  $\hbar \rightarrow \chi$ ,  $m \rightarrow 1$ ,  $R \rightarrow 1$ , and  $\epsilon \rightarrow 1$ . In direct analogy with Eq. (7b) we find

$$\partial_t \rho + \partial_\theta (\rho \tilde{v}) = 0 \quad (9a)$$

$$\partial_t \tilde{v} + \tilde{v} \partial_\theta \tilde{v} + \partial_\theta \Phi = \partial_\theta \left( \frac{\chi^2}{2} \frac{\partial_\theta^2 \sqrt{\rho}}{\sqrt{\rho}} \right) \quad (9b)$$

where  $\Psi = \sqrt{\rho} e^{i\tilde{S}/\chi}$ , and  $\tilde{v} = \partial_\theta \tilde{S}$  is the appropriately scaled velocity-profile.

## C. Connection to Classical Analysis

### 1. Classical Mean-Field Description

The classical mean-field description of the HMF model is given by the Vlasov, or collisionless Boltzmann, equation. This dictates the evolution of the phase space density  $f(\theta, p, t)$  via the conservation law

$$\frac{d}{dt} f = \partial_t f + \dot{\theta} \partial_\theta f + \dot{p} \partial_p f = 0. \quad (10)$$

We can identify  $\dot{x} = p/m$  and  $\dot{p} = F$ . Additionally due to the additive long-range nature of the cosine potential, the

force experienced by a single particle can be expressed as the gradient of the mean-field potential via  $F = \partial_\theta \Phi$ .

Generally there will be some finite velocity-dispersion, however in the special case where each point in space can be assigned a definite velocity, the equations can be written in terms of a density-profile,  $\rho(\theta, t)$ , and a velocity-profile  $v(\theta, t)$  [17]. In terms of these variables the equations take the form

$$\partial_t \rho + \frac{1}{R} \partial_\theta (\rho v) = 0 \quad (11a)$$

$$\partial_t v + \frac{1}{R} v \partial_\theta v + \frac{\epsilon}{mR} \partial_\theta \Phi = 0 \quad (11b)$$

and can be interpreted as the equations of motion for a classical fluid.

### 2. Semi-Classical Limit

Although the mean-field treatment assumed for this entire section is often referred to as a classical approximation in the BEC literature, we will reserve the word classical for the  $\hbar \rightarrow 0$  limit.

Eqs. (4b) and (9b) emphasize that, up to dilations in time, the dynamics of the system are controlled entirely by the parameter  $\chi^2$ . It follows that the semi-classical limit can therefore be defined entirely in terms  $\chi^2$ . Inspecting the proportionality relation  $\chi^2 \propto \hbar^2$  it is clear that the semi-classical regime occurs when  $\chi^2 \ll 1$ , or equivalently when  $\chi^{-2} \gg 1$ . In the language of Eq. (4b) this statement implies a very deep mean-field potential, while for Eq. (9b) the classical limit amounts to the removal of the quantum pressure.

Re-writing Eq. (4a) explicitly in terms of the magnetization yields

$$i\partial_\tau \Psi = -\partial_\theta^2 \Psi + 2\chi^{-2} M \cos(\theta - \varphi) \Psi. \quad (12)$$

It is now manifest that  $\chi^{-2} \gg 1$  is a necessary, but not sufficient, condition to ensure a suitably deep potential over the course of dynamics. It is actually the combination  $\chi^{-2} M$  which dictates the depth of the potential, and therefore the relative size of classical, compared to quantum effects. The magnetization's evolution is sensitive to the initial configuration of the order-parameter, and although the  $\hbar \rightarrow 0$  limit can be taken in the limit of vanishing  $M$ , this is equivalent to a rescaling of time and does not correspond to a qualitative difference in the system's dynamics.

We can also explore classicality with the help of Eq. (9b). We can see that in the  $\chi \rightarrow 0$  limit these fluid equations are equivalent to those found in Eq. (11b). It follows that the quantum mean-field description for pure-states is equivalent to the classical mean-field description, but only in limit of vanishing velocity dispersion. The idea of a classicality condition independent of  $M$ , would seem to contradict the previous paragraph, however in

the case of a small, or vanishing,  $M$  the dynamics will still be dominated by free-Schrödinger evolution. The “classicality” will be equivalent to a re-scaling of the dynamical time-scale, and so does not represent any qualitative change in the model’s dynamics.

#### D. Connection to the Micro-Cannonical Ensemble

Classical analysis of the HMF has traditionally tried to connect dynamical simulations with statistical predictions of the micro-cannonical ensemble. To make contact with classical analysis it is therefore important to establish the connection between the internal energy in the classical HMF model, and the average energy for a quantum state.

We have shown the equivalence of the quantum and classical theories for  $\chi = 0$  using the hydrodynamical variables  $u$  and  $\rho$  so it makes sense to express both the classical, and quantum energies in terms of these variables.

The GGPE conserves both energy, and particle number. To emphasize the connection to the classical energy we will follow Ref. [12] and write the energy functional corresponding to Eq. (8)

$$E[\Psi] = \int \frac{|\chi|^2}{2} |\partial_\theta \Psi|^2 d\theta + \frac{1}{2} \int \int |\Psi(\theta')|^2 \cos(\theta - \theta') |\Psi(\theta)|^2 d\theta d\theta'. \quad (13)$$

Re-writing the equation in terms of the hydrodynamic variables  $\tilde{v}$  and  $\rho$ , and referring to Eq. (5c) we find

$$E[\Psi] = \int \frac{1}{8} \chi^2 \frac{(\partial_\theta \rho)^2}{\rho} d\theta + \frac{1}{2} \int \rho \tilde{v}^2 d\theta + \frac{1}{2} M^2[\Psi] \quad (14)$$

$$E[\Psi] = E_Q + T_{Cl} + U_{Cl}$$

which agrees with the classical result for a dispersionless velocity profile with an additional correction that is proportional to  $\chi^2$  and the curvature of the density profile. In this way we can identify a measure of the importance of quantum effects at a given time in the system’s evolution

$$\frac{|E_Q|}{T_{Cl}^2 + U_{Cl}^2} \quad (15)$$

which can give us some indication of the importance of quantum effects throughout the dynamics.

### III. ANALYTIC RESULTS

#### A. Stationary Solutions

Although we are primarily concerned with the dynamics of the HMF model, an understanding of the stationary solutions of the model is also important. We begin by searching for solutions with a time-independent

density-, and velocity-profile. These can be expressed as  $\Psi(\theta, \tau) = \psi(\theta) e^{-i\mu\tau}$  with no loss of generality. The time-independence of the order-parameter implies a time independent mean-field potential. This means that both  $M$  and  $\varphi$  can be taken as constant. By choosing our coordinates appropriately we can set  $\varphi$  to zero. Proceeding as outlined above, and using Eq. (4a) we arrive at a nonlinear eigenvalue problem

$$\mu\psi = (-\partial_\theta^2 + 2\chi^{-2} M[\psi] \cos \theta) \psi \quad (16)$$

which can be mapped to the Mathieu equation. Using the notation found in Ref. [18] the Mathieu equation is expressed as

$$\partial_z^2 w + (a - 2q \cos(2z))w = 0. \quad (17)$$

Making the identification  $z = 2\theta$  leads to  $\partial_z^2 \rightarrow 1/4 \partial_\theta^2$ . Renormalizing Eq. (17) we can then identify  $a = 4\mu$ , and  $4q = M\chi^{-2}$ .

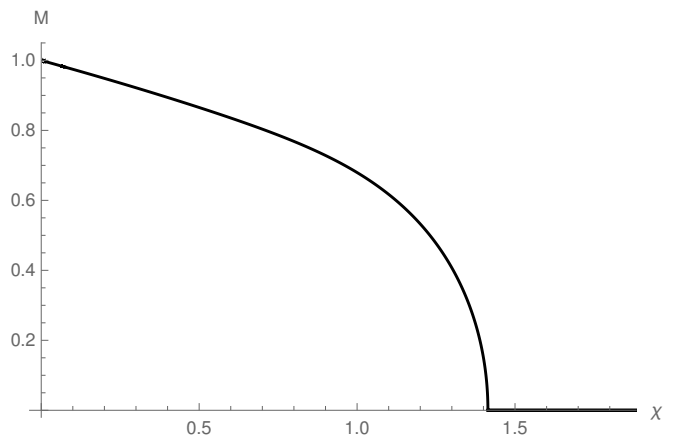


FIG. 1. Magnetization vs  $\chi$  calculated using the self-consistent procedure involving Mathieu functions; compare with Figure 5 of Ref. [12].

The solutions of the Mathieu equation can be partitioned into even and odd functions denoted  $ce_n(z, q)$  and  $se_n(z, q)$  respectively with associated eigenvalues  $a_n$  and  $b_n$ . It is important to note that these functions are only  $\pi$  periodic in  $z$ , and therefore  $2\pi$  periodic in  $\theta$ , for  $n$  even. Our system is defined on a ring, and therefore has periodic boundary conditions so we must necessarily restrict ourselves to  $n$  even.

For any given Mathieu function we can compute the magnetization. Referring to Eq. (5c) and noting that  $M = M$  in our chosen set of coordinates we have

$$M_n(q) = \int_{-\pi}^{\pi} |\psi_n(\theta, q)|^2 \cos(\theta) d\theta \quad (18)$$

and we know that  $4q = M\chi^{-2}$ . With the help of *Mathematica* we can solve for  $\chi^{-2}(q)$  for any Mathieu function  $se_{2n}$  or  $ce_{2n}$  and then invert the function to find  $q(\chi^{-2})$ . This allows one to characterize all of the possible stationary solutions of the GGPE for the HMF model. It

should be noted that  $A * e^{in\theta} + B e^{-in\theta}$  is stationary for all values of  $\chi^2$ .

The special case of the minimum energy configuration of Eq. (16) was solved in Ref. [12] by the use of a shooting method. Our method has the advantage that it supplies an analytic form for the mean-field ground state, and that it allows one to find other stationary states. As a confirmation of this method we have reproduced two of Chavanis' figures, Figs. 1 and 2.

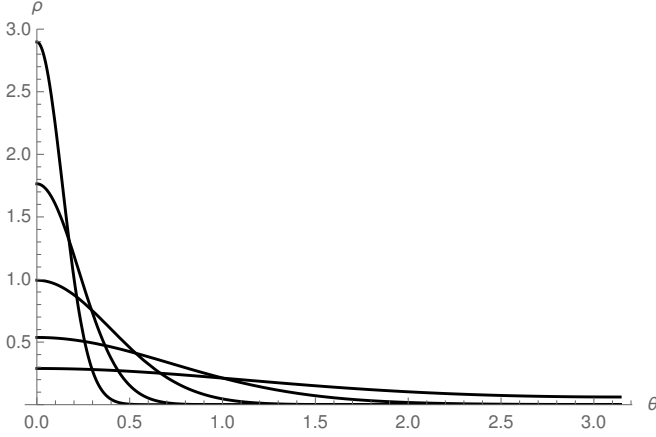


FIG. 2. Ground state calculated with Mathieu functions for  $\chi \in \{1.33, 0.85, 0.3, 0.1, 0.376\}$  (from top to bottom); compare with Figure 8 of Ref. [12].

### B. Linearized Quantum Dynamics

Taking Eq. (9b) and linearizing about a spatially homogeneous density  $\rho_0 = \frac{1}{2\pi}$ , with  $\rho = \rho_0 + \rho_1$  and  $\tilde{v} = \tilde{v}_1$  yields

$$\partial_{\mathcal{T}} \rho_1 + \rho_0 \partial_{\theta} \tilde{v}_1 = 0 \quad (19a)$$

$$\partial_{\mathcal{T}} \tilde{v}_1 = -\partial_{\theta} \left( \Phi[\rho_1] + \frac{\chi^2}{4\rho_0} \partial_{\theta}^2 \rho_1 \right). \quad (19b)$$

Decomposing the linear perturbations into Fourier modes,  $\rho_1 = \sum \alpha_k(\mathcal{T}) e^{ik\theta}$  and  $\tilde{v}_1 = \sum a_k(\mathcal{T}) e^{ik\theta}$  leads to the following set of equations

$$\partial_{\mathcal{T}} \alpha_k = -ik \rho_0 a_k \quad (20a)$$

$$\partial_{\mathcal{T}} a_k = -ik(\pi \delta_{k,-1} - \pi \delta_{k,1} - \frac{\chi^2}{4\rho_0} k^2) \alpha_k. \quad (20b)$$

These equations were considered by Chavanis in his stability analysis [12], and are a quantum generalization of those studied by Barré *et. al.* to explain the appearance of long-lived cheverons in the density profile of the classical model [1].

These equations can be re-arranged to obtain dispersion relations for the linear-profiles' Fourier modes. These are given by

$$\omega_k^2 = \frac{1}{2} \left( \frac{1}{2} \chi^2 k^4 \pm \delta_{|k|,1} k^2 \right) \quad (21)$$

with the upper sign corresponding to repulsive interactions, and the lower sign corresponding to attractive interactions [12]. We see that the  $|k| \neq 1$  modes undergo free evolution. In the classical limit, all  $|k| \neq 1$  modes must vanish, or they will grow linearly in time. This is because, for the classical HMF model, the right-hand side of Eq. (20b) vanishes, implying constant  $a_k$ , but if  $a_k = C \neq 0$  then  $\alpha_k = ikCt$ . This is not the case with the inclusion of quantum effects, where the quantum pressure stabilizes these modes, and leads to oscillatory solutions.

Assuming initial data with  $a_k = 0 \forall k \notin \{-1, 0, 1\}$ , the analysis in Sec. 2.2 of Ref. [1] remains valid provided the frequency is re-scaled in accordance with Eq. (21). This essentially involves the substitution of the ansatz  $\tilde{v} = (A\omega) \sin(\omega\mathcal{T}) + Au(\overline{\mathcal{T}})$ , with  $\overline{\mathcal{T}} = A\mathcal{T}$ , into Eq. (9b). This is motivated by the assumption that the characteristic time scale of the non-linear dynamics is much longer than that of the linear dynamics, and that their ratio is proportional to the amplitude of the initial perturbation. Proceeding we obtain

$$\begin{aligned} A^2 \partial_{\overline{\mathcal{T}}} u + \frac{\omega^2 A^2}{2} \sin(2\theta) \sin^2(\omega\mathcal{T}) + A^2 u \partial_{\theta} u + \omega A^2 [\sin \theta \partial_{\theta} u + u \cos \theta] \sin(\omega\mathcal{T}) \\ = \underbrace{\int_{-\pi}^{\pi} \rho(\theta', \mathcal{T}) \sin(\theta - \theta') d\theta'}_L - \partial_{\mathcal{T}} v + \underbrace{\partial_{\theta} \left( \frac{\chi^2}{2} \frac{\partial_{\theta}^2 \sqrt{\rho}}{\sqrt{\rho}} \right)}_{QP}. \end{aligned} \quad (22)$$

Note the left-hand side of the equation is proportional to  $A^2$ . Next averaging over the short time-scale  $\mathcal{T}$  the bracketed term is set to zero, and  $\sin^2(\omega\mathcal{T}) \rightarrow 1/2$ . This

leads us to

$$\partial_{\overline{\mathcal{T}}} u + u \partial_{\theta} u = -\frac{\omega^2}{4} \sin 2\theta + A^{-2}(L + QP) \quad (23)$$

In the classical limit  $QP \rightarrow 0$ , and in the analysis of Barré *et. al.*  $L$  is assumed to vanish. This ansatz is vindicated by comparison with exact numerical simulations and therefore would seem to hold up to at least  $\mathcal{O}(A^3)$ .

It is unclear whether or not the quantum potential will be negligible. Even if it is small at early times, classical analysis suggests that hyperdense caustics (see Section IV C) would emerge. These have very high curvature, and therefore would dynamically induce a strong quantum pressure. We will revisit this question in Section IV.

## IV. NUMERICAL RESULTS

### A. Numerical Method

To solve the evolution of the GGPE we used the representation of Eq. (5c). This approach was advantageous because, unlike a generic two-body potential, the cosine potential only couples adjacent momentum modes. This leads to a tri-diagonal pseudo-Hamiltonian,  $H_{kk'}(\tau)$ , whose time dependence is inherited from the evolution of the order parameter by way of the mean-field potential. We used a second-order integration scheme based on the Dyson series, and would abort simulations in which the particle number or energy, varied by more than one part per thousand. Essentially we defined a time evolution operator  $U_{kk'}[a_k]$ , whose local error scales like  $\Delta\tau^3$ , and solved the difference equation

$$a_k(\tau_{i+1}) = U_{kk'}(\tau_i)a_{k'}(\tau_i). \quad (24)$$

iteratively for  $i \in \{1, \dots, i_{\max}\}$ . Implicit schemes were also tested, and gave indistinguishable results.

### B. Spontaneous Breaking of the Reflection Symmetry

The HMF model's time evolution operator is a function of the pseudo-Hamiltonian, and therefore inherits its symmetries. Initial data whose density is even in  $\theta$ , will therefore have its density remain even in  $\theta$  throughout its evolution.

While this has been the case in the majority of simulations, for certain initial configurations the symmetry can be broken by a violent focussing. Specifically when a very small density wave, with  $k = 1$  is added on top of a uniform background a long-period of free-Schrödinger evolution ensues, followed by a dynamical breaking of the reflection symmetry. This would seemingly point to an instability in the system.

This is the same initial configuration that leads to the well studied bi-cluster under classical evolution, however here there are two major qualitative differences. First, there is only one set of chevrons. Secondly the time-scale separating subsequent chevrons from one another is very

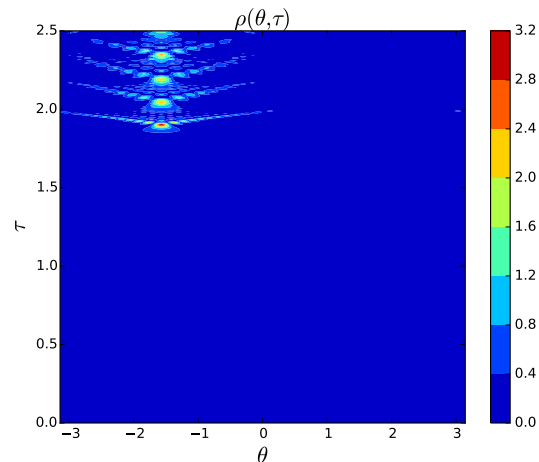


FIG. 3. Emergence of a single cluster from a homogeneous background with small density wave. Initial conditions were selected to match those in Ref. [1]. Although the initial conditions were even in  $\theta$  the symmetry is broken dynamically.

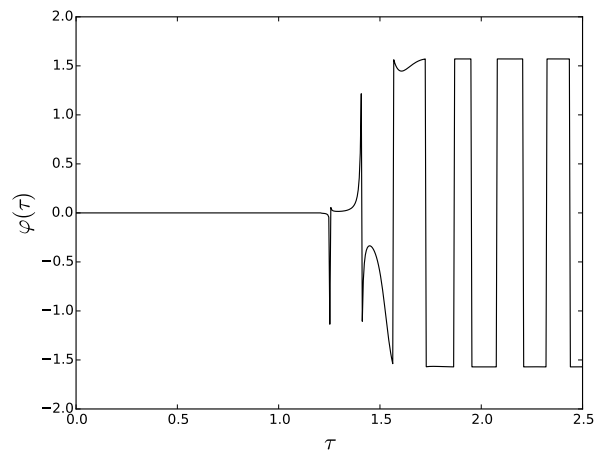


FIG. 4. Minimum of the mean-field potential  $\Phi$  as a function of time. We can see that the reflection symmetry is preserved until  $\tau \sim 1.2$ . Note the symmetry breaking appears much earlier here than in the density profile. The discontinuities are points where the magnetization has changed sign. At late times the potentials minimum/maximum stays fixed and it oscillates from attracting and repulsing the cluster.

different than the time-scale in which the first chevron formed. This is in contrast to the classical case where these two time-scales are intimately linked [1].

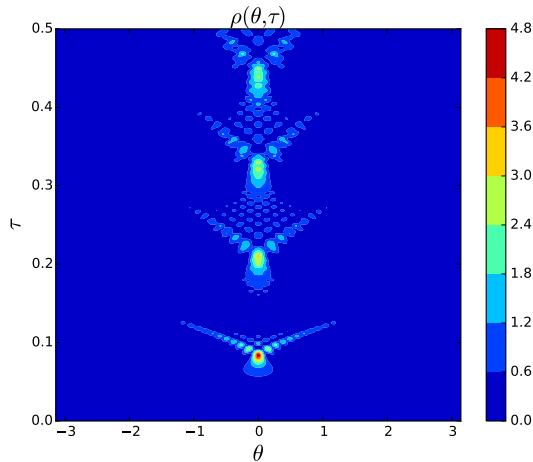


FIG. 5. Density profile evolution for  $\chi^{-2} = 300$ . Initial data has a cosine component and a uniform component. Note the intense focussing and cuspy profile of the focussing.

### C. Appearance of the Pearcey Function

#### 1. Chevrons in the Classical HMF Model

One of the features of the classical HMF model that attracted considerable interest was the appearance of long-lived out-of-equilibrium structures. These were termed chevrons, and received a theoretical explanation where they were shown to result from an effective potential which is generated by a combination of non-linear effects, and linear plasma oscillations [1].

Although the original observations of this phenomena involved simulations with a water-bag initial distribution, it was in the limit of small velocity dispersion that the chevrons were most pronounced. This led to their treatment in a zero-temperature approximation, where they were found to result from a pile-up of characteristics resulting from a forced Burger's equation. It is this realization that makes catastrophe theory the natural language in which to discuss these features. In fact, the approach used in Ref. [1] to determine the shape of the caustics (Sec 3.1 specifically) is a textbook example of the theory at work.

Catastrophe theory applies to entities defined by a gradient map, which defines a family of rays (to borrow the language of optics). In the case of the HMF model this mapping is the extremization of the action, and the corresponding rays are the characteristics of the velocity profile, or the trajectories of individual particles in a molecular dynamics simulation.

The theory also asserts that any singularity resulting from a pile-up of these rays, that is not the result of fine tuning, can be classified into equivalence classes. It also asserts that in the local vicinity of the singularity the structure of the density is universal, and in the case of the HMF model, the prediction is that all singularities

will form as either fold or cusp catastrophes, and this has been confirmed explicitly [1]. Finally these universal structures are guaranteed to be robust against perturbations, and should therefore be expected to survive changes to the parameters of the system [19].

Wave theories whose semi-classical, or short wavelength, limit yields a gradient map (theory of rays) display related universal behaviour in the vicinity of their corresponding ray's singularities. A well known example of this is the Airy function, whose short wave-length limit tends to a fold catastrophe. The wave-regulated version of the cusp catastrophe also has an associated special function, and is known as the Pearcey function, and has been studied since its introduction in optics over sixty years ago and its properties are well tabulated [18]. It can be defined in terms of the diffraction integral shown below.

$$Pe(x, y) = \int_{-\infty}^{\infty} e^{i(t^4 + xt^2 + yt)} dt \quad (25)$$

The fact that the behaviour of the system's dynamics can be categorized in a universal fashion, and that the appearance of universal special functions can be predicted by analyzing the simpler ray-theory, makes catastrophe theory a powerful tool. Below we will show how these cusps appear in the ferromagnetic case of the HMF.

#### 2. Numerical Results and Comparison with Classical Trajectories

To study the appearance of the Pearcey function it is advantageous to study the ferromagnetic case of the HMF model. This is because the repulsive interactions work in conjunction with the quantum pressure to disfavour large modulations in the density profile. This often leads to a suppression of the magnetization, which causes a shallow potential to emerge, and free-Schrödinger-like evolution to dominate the dynamics.

In contrast the attractive mean-field potential encourages large density modulation and competes directly with the quantum pressure. This allows for violent focussing. This is very different from the classical caustics studied in [1, 3], which we have been unable to reproduce in the quantum dynamics (see Section IV B).

To confirm that the focussing in the density profile corresponds to envelopes of a family of rays in the classical theory, we note that knowing the evolution of the mean-field potential  $\Phi$  *a posteriori* we can map our non-linear problem, onto a linear single-particle system with time varying potential  $V(\theta, \tau) = \Phi(\theta, \tau)$ . The corresponding classical rays are given by solving the characteristics of the Hamilton-Jacobi equation. The initial density of rays was chosen to correspond to a sampling of the initial data's density function  $\rho_0$ , and initial conditions were chosen so that the initial velocity profile was uniform, and vanishing. The results are shown in Fig. 7. Comparing with Fig. 5 we see that the appearance of the

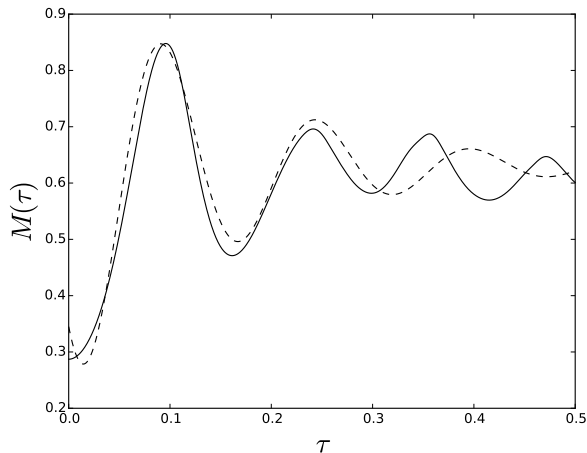


FIG. 6. Comparison of numerics (solid line) vs the ansatz (dashed) used as an input for the classical trajectories plotted in Fig. 7. Although there are clearly small discrepancies, catastrophes are robust against perturbations.

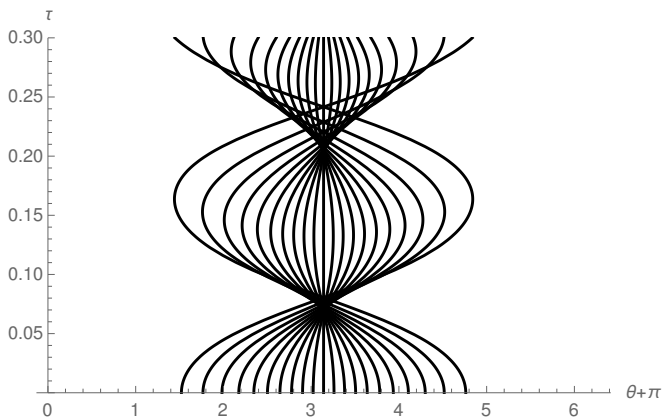


FIG. 7. Trajectories of particles computed by solving Newton's equations for a particle travelling in a cosine potential whose amplitude varies as shown in Fig. 6.

over-dense regions is well predicted by the trajectories, and this suggests that what is seen in Fig. 5 is a wave-regulated catastrophe, whose local wave-function can be predicted on general grounds.

## V. CONCLUSIONS AND FUTURE WORK

A method for calculating all of the stationary states of the HMF model's mean-field dynamics was derived. The method is exact and makes use of Mathieu functions. We confirmed the method reproduced previous work. Initial data that lead to caustics under classical evolution, was evolved with the GGPE and found to display focussing

that was qualitatively different from the classical case, most strikingly in that it spontaneously broke the initial data's reflection symmetry. We explored the connection between the caustics observed classically, and the Pearcey function in the semi-classical limit and showed that over-dense regions can be interpreted as wave regulated caustics, which arise from a pile-up of trajectories that are generated by the mean-field potential. With catastrophe theory's guarantees of universality, and stability, these over-dense regions' density profile can be argued to take the form of a special function in the immediate vicinity of the caustic.

One interesting feature of this work is the fact that the mean-field limit ( $N \rightarrow \infty$ ) for pure-states cannot reproduce certain aspects of classical many-body behaviour, namely finite-velocity dispersion. An interesting question one could ask is: Could many-body states with quantum fluctuations in the phase mimic the effects of non-zero velocity dispersion? These questions have been partially answered by Chavanis, who showed that the Wigner equation, when linearized around a homogeneous background, reproduces the linearized Vlasov equation [12]. These questions are beyond the scope of our mean-field analysis, never the less they are potentially interesting avenues of investigation for future work.

Additionally the validity of the mean-field approximation for long-range interacting quantum many-body systems is an obvious issue that must be addressed. Although rigorous proofs exist for the correspondence between N-body dynamics, and the Vlasov equation for classical systems, it is unclear at what level the mean-field approximation is valid for the quantized HMF, especially given its low dimensionality.

Prospects for studying the quantum HMF model are especially promising. Work in the cold atoms community has shown that there may be hope of realizing this model in a laboratory [20], however such a realization would be inherently quantum, and so a deeper understanding of the model's dynamics is essential. This includes many-body effects that go beyond the mean-field theory.

## THANKS AND ACKNOWLEDGEMENTS

This research was supported by funds from the Ontario Graduate Scholarship (OGS) program, and the National Science and Engineering Research Council.

This research was supported in part by Perimeter Institute for Theoretical Physics. Research at Perimeter Institute is supported by the Government of Canada through the Department of Innovation, Science and Economic Development and by the Province of Ontario through the Ministry of Research and Innovation.



- 
- [1] J. Barré, F. Bouchet, T. Dauxois, and S. Ruffo, *Physical Review Letters* **89**, 110601 (2002).
  - [2] M. Antoni and S. Ruffo, *Physical Review E* **52**, 2361 (1995).
  - [3] T. Dauxois, V. Latora, and A. Rapisarda, *Dynamics and ...*, 458 (2002).
  - [4] A. Campa, T. Dauxois, and S. Ruffo, *Physics Reports* **480**, 57 (2009), arXiv:0907.0323.
  - [5] F. Staniscia, P. H. Chavanis, and G. De Ninno, *Physical Review E* **83**, 051111 (2011).
  - [6] T. Dauxois, S. Ruffo, E. Arimondo, and M. Wilkens, eds., *Dynamics and Thermodynamics of Systems with Long Range Interactions* (Springer-Verlag, Berlin Heidelberg, 2002) p. 492.
  - [7] A. Figueiredo, T. M. D. R. Filho, and M. A. Amato, *EPL (Europhysics Letters)* **83**, 30011 (2008), arXiv:0805.1568v1.
  - [8] A. C. Ribeiro-Teixeira, F. P. C. Benetti, R. Pakter, and Y. Levin, *Physical Review E - Statistical, Nonlinear, and Soft Matter Physics* **89**, 1 (2014), arXiv:1202.1810 [cond-mat.stat-mech].
  - [9] F. A. Tamarit, G. Maglione, D. A. Stariolo, and C. Anteneodo, *Physical Review E - Statistical, Nonlinear, and Soft Matter Physics* **71**, 1 (2005).
  - [10] C. Anteneodo and F. A. Tamarit, *Physica A: Statistical Mechanics and its Applications* **371**, 135 (2006).
  - [11] C. B. Tauro, C. G. Maglione, and F. a. Tamarit, *Journal of Physics: Conference Series* **246**, 012020 (2010).
  - [12] P.-H. Chavanis, *Journal of Statistical Mechanics: Theory and Experiment* **2011**, P08003 (2011).
  - [13] P.-H. Chavanis, *Journal of Statistical Mechanics: Theory and Experiment* **2011**, P08002 (2011).
  - [14] C. J. Pethick and H. Smith, *Bose-Einstein condensation in dilute gases* (Cambridge university press, 2002).
  - [15] W. Braun and K. Hepp, *Communications in Mathematical Physics* **56**, 101 (1977).
  - [16] L. L. Foldy, *Physical Review* **124**, 649 (1961).
  - [17] J. Barré, F. Bouchet, T. Dauxois, and S. Ruffo, *The European Physical Journal B - Condensed Matter* **29**, 577 (2002), arXiv:0203013 [cond-mat].
  - [18] F. W. J. Olver, D. W. Lozier, R. F. Boisvert, and C. W. Clark, *Book*, Vol. 5 (Cambridge University Press, 2010) p. 966.
  - [19] M. V. Berry, "Singularities in waves and rays," (1980).
  - [20] S. Schütz and G. Morigi, *Physical Review Letters* **113**, 203002 (2014).